

Conditioning DRASTIC model to simulate nitrate pollution case study: Hamadan–Bahar plain

Samira Akhavan · Sayed-Farhad Mousavi ·
Jahangir Abedi-Koupai · Karim C. Abbaspour

Received: 26 May 2009 / Accepted: 4 October 2010 / Published online: 20 October 2010
© Springer-Verlag 2010

Abstract One of the major causes of groundwater pollution in Hamadan–Bahar aquifer in western Iran is a non-point source pollution resulting from agricultural activities. Withdrawal of over 88% of drinking water from groundwater resources, adds urgency to the studies leading to better management of water supplies in this region. In this study, the DRASTIC model was used to construct groundwater vulnerability maps based on the “intrinsic” (Villeneuve et al. 1990). This is especially true in arid and (natural conditions) and “specific” (including management) concepts. As DRASTIC has drawbacks to simulate specific contaminants, we conditioned the rates on agricultural activities. In Hamadan, western Iran, measured nitrate data and optimized the weights of the specific intensive agriculture, traditional methods of handling sewage, slaughterhouses, and animal farming are principal causes of water pollution on a regional scale. Increasing population has improved significantly ($R^2 = 0.52$) over the intrinsic ($R^2 = 0.12$) and specific ($R^2 = 0.19$) models in predicting the groundwater nitrate concentration. Our study suggests that a locally conditioned DRASTIC model is an effective tool for predicting the region’s vulnerability to nitrate pollution. In addition, comparison of groundwater tables between two periods 30 years apart indicated a drawdown of around 50 m in the central plain of the Hamadan–Bahar region. Our interpretation of the vulnerability maps for the region. As drinking water supply comes mainly from central valley requiring careful evaluation and monitoring, groundwater sources, this adds urgency to the study of ways to protect public water supplies of the region.

S. Akhavan · S.-F. Mousavi · J. Abedi-Koupai
Department of Water Engineering,
Isfahan University of Technology,
College of Agriculture, 84156-83111 Isfahan, Iran

K. C. Abbaspour (✉)
Eawag, Swiss Federal Institute of Aquatic Science
and Technology, 8600 Dübendorf, Switzerland
e-mail: abbaspour@eawag.ch

Groundwater vulnerability mapping is based on the idea that some land areas are more vulnerable to groundwater contamination than others (Gogu and Dassargues 2000). This provides useful information to protect groundwater resources and to evaluate the potential for water quality improvement with changes in agricultural practices and land use applications (Almasri 2008).

Vulnerability is usually considered as an intrinsic property of a groundwater system that depends on its

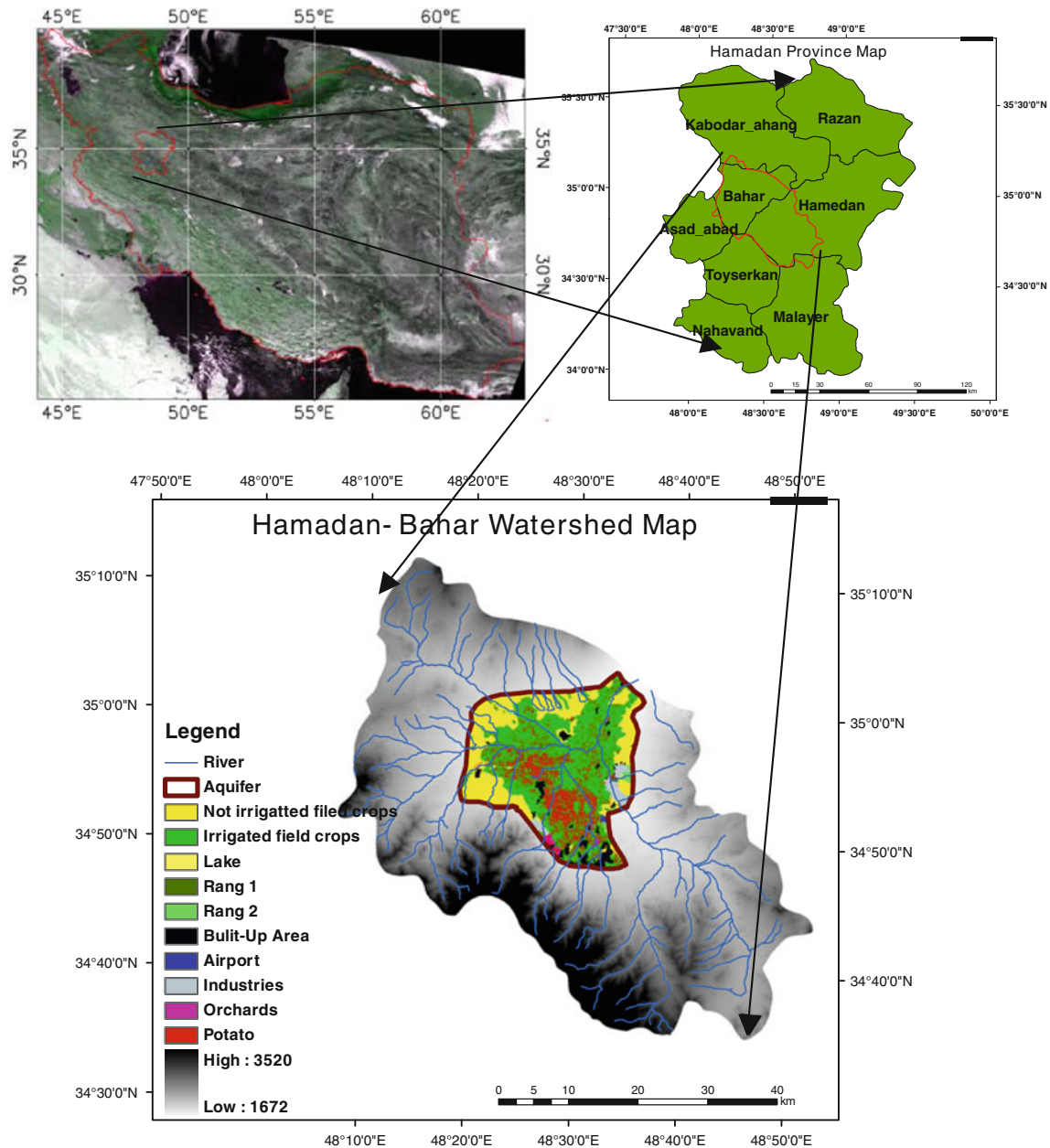


Fig. 1 Study area of Hamadan–Bahar plain in Hamadan province, Iran

sensitivity to natural impacts. Specific or integrated vulnerability with the risk of the groundwater being exposed to the loading of pollutants from certain man-made sources (Vrbassess groundwater vulnerability to a wide range of potential contaminants (Al-Adamat et al. 2003, Almasri and Zaporozed 1994, Babiker et al. 2005). Groundwater models often have data requirements that cannot be satisfied in many parts of the world (Al-Adamat et al. 2003). The attraction of the vulnerability concept is that it is implemented by classifying a geographical area with regard to its susceptibility to groundwater contamination. Various techniques and methodologies have been developed to evaluate environmental impacts associated with recharge potential (R), aquifer media (A), soil media

(S), topography T), impact of vadose zone I) (and hydraulic conductivity C) of the aquifer. Landuse was added to the above system by Secunda et al. 1990 to produce the so-called “speci c” vulnerability index. Advantage of the DRASTIC model is that it uses a relatively small number of parameters to compute the vulnerability index, which ensures the best representation of the hydrogeological setting. This makes the model suitable for producing comparable vulnerability maps on a regional scale (Babiker et al. 2005).

Panagopoulos et al. 2006 investigated several studies using the DARSTIC model and reported on some perceived disadvantages such as many variables being factored into one nal index (Vrba and Zaporozec 1994; Merchant 1994, 1989), exclusion of many important scienti cally de ned factors such as sorption capacity, travel time and dilution and general dif culty of testing the model (Rose 1994).

Despite these criticisms, many advantages of the DRASTIC model have also been recognized including: the method’s low cost of application (Aller et al. 1987), and the relative accuracy of model results for extensive regions with a complex geological structure (Kalinski et al. 1994; McLay et al. 2001). In fact, information gained by modeling at different levels of complexities can complement each other and lead to a better understanding of the system under study.

DRASTIC has been applied to many regions around the world, including Tehran–Karaj aquifer, located in central Iran, to classify aquifer vulnerability using fuzzy system (Mohammadi et al. 2008), Kherran plain in Khuzestan (south west of Iran), to construct a groundwater vulnerability map (Chitsazan and Akhtari 2008), Metline-Ras Jebel-Raf Raf aquifer, north east of Tunisia, to classify aquifer vulnerability maps (Hamza et al. 2007), and Kaka-migahara Heights, Gifu Prefecture, Central Japan, to estimate aquifer vulnerability and demonstrate the combined use of the DRASTIC and GIS (Babiker et al. 2005).

Few attempts have been made to validate and verify the performance of a DRASTIC model as it is usually applied to areas of no data availability. An exception is the study of Panagopoulos et al. 2006 who modi ed the rates and optimized the weights of a DRASTIC model based on the correlation of each parameter with measured nitrates concentrations in groundwater. But there is an intrinsically high degree of uncertainty in this type of evaluation because pollutant loads are the consequence of complex interactions between environmental, landscape, and anthropogenic factors.

The objectives of this study are to determine the vulnerability of aquifers in Hamadan–Bahar plain with the intrinsic and speci c DRASTIC models and to show a simple procedure for training the model on a certain contaminant, in this case nitrate. The training is performed by conditioning the rates and optimizing the weights of the

DRASTIC model on measured nitrate concentrations. ArcGIS (Ver. 9.2) was used to facilitate the analysis and Sequential Uncertainty Fitting (SUF12, Ver. 2) (Abbaspour et al. 2007) was applied for optimization of the weights.

Materials and methods

Description of the study area

Hamadan–Bahar aquifer is located in Hamadan province, Iran (Fig. 1). The study area lies between longitudes 48°33'E and latitudes 34°49'N and 35°02'N. The total area of Hamadan–Bahar aquifer is 480² km² and the aquifer is unconfined. Geologically, Hamadan–Bahar aquifer is located on Sanandaj–Sirjan metamorphic zone (Hamadan Regional Water Authority, HRWA). The parent rocks are mainly limestone, calcareous shale and granitic material.

The oldest deposits contain slate and schist from Jurassic age that outcrop in the eastern and southern parts of the basin. The Cretaceous deposits consist of the carbonate series. The main portion of the study area is covered by Quaternary sediments and consists mainly of recent alluvium and conglomerate. Hamedan–Bahar alluvial aquifers consist mainly of gravel, sand, silt and clay. The alluvial sediment thickness varies from 25 m in the sides to 75 m in the center of the plain.

The transmissivity of the Hamadan–Bahar ranges from 100 to 1,750 m² day⁻¹, while the speci c yield of the aquifer is about 5–10%. Groundwater supplies approximately 88% of the water consumed in Hamadan. The region has a cold semi-arid climate with an average annual pre-cipitation of 325 mm and mean annual temperature of 11 °C.

The main agricultural crops in Hamadan–Bahar plain include wheat and potato. In recent years, large amounts of chemical and animal fertilizers are applied to boost crop production, the consequence of which is large nitrate concentration in groundwater exceeding the standard limits.

Table 1 summarizes the annual amount of N-fertilizers applied in Hamadan and Bahar agricultural lands for potato according to the data from the Information Center of Hamadan and Bahar regions during 2004–2007

| Fertilizer | 2004–2005 | 2005–2006 | 2006–2007 | Mean |
|------------------------------------|-----------|-----------|-----------|------|
| Hamadan | | | | |
| Urea (kg ha ⁻¹) | 791 | 905 | 301 | 666 |
| Hen manure (ton ha ⁻¹) | 28 | 21 | 24 | 24 |
| Bahar | | | | |
| Urea (kg ha ⁻¹) | 390 | 482 | 393 | 422 |
| Hen manure (ton ha ⁻¹) | 9 | 15 | 10 | 11 |

Ministry of Jahade-Agriculture of Hamadan. For wheat, an average of 150 kg ha⁻¹ urea is applied in these regions.

DRASTIC model and model calibration

DRASTIC is an overlay-and-index method that was developed for the US Environmental Protection Agency by the American Water Well Association (Aller et al. 1987). But it has since become a widely used model around the world. DRASTIC is a conceptual model defined as a composite description of the most important geological and hydrological factors that could potentially affect groundwater pollution. The model yields a numerical index that is derived from ratings and weights assigned to the seven model parameters expressed as follows:

$$V_{intrinsic} = D_r D_w + R_r R_w + A_r A_w + S_r S_w + T_r T_w + I_r I_w + C_r C_w \tag{1}$$

where $V_{intrinsic}$ is the intrinsic vulnerability, $D, R, A, S, T, I,$ and C are the seven parameters defined in Table 2, and the subscripts r and w stand for rate and weight, respectively.

The intrinsic DRASTIC method gives the vulnerability of groundwater against any pollution of surface origin, independent of the landuse or any actual occurrence of pollutants. In a modification, Secunda et al. (1998) added landuse to the model and estimated the specific vulnerability as follows:

$$V_{specific} = V_{intrinsic} + L_r L_w \tag{2}$$

where $V_{specific}$ is the specific vulnerability, and L_r and L_w are landuse rate and weight, respectively.

The recharge rates and weights used here were based on those proposed by Pisco (2001) and the landuse rates and weights were based on those published by Secunda et al. (1998). The remaining parameter weights and rates were based on those suggested by Aller et al. (1987). The DRASTIC parameters were manipulated as raster maps in an ArcGIS environment (Ver. 9.2).

For the purposes of this research, the intrinsic and specific vulnerability indices were conditioned on observed nitrate concentrations of the aquifers in the region of study. To do this, both rates and weights were redefined. For new rates of categorical variables, first the average nitrate concentration was calculated for each category and then used in the following equation:

$$r(v)_j = \frac{[NO_3^-]_{avg,j}}{[NO_3^-]_{avg}} \times 10 \times \left\{ \text{MAX}_{j=1..J} \left[\frac{[NO_3^-]_{avg,j}}{[NO_3^-]_{avg}} \right] \right\}^{-1} \tag{3}$$

where $r(v)_j$ is modified rate for the j th category ($j = 1, \dots, J$), $[NO_3^-]_{avg,j}$ is the average of nitrate concentration for the j th category, $[NO_3^-]_{avg}$ is the average nitrate concentration over all categories ($mg\ l^{-1}$), and MAX is the maximum of $\frac{[NO_3^-]_{avg,j}}{[NO_3^-]_{avg}}$ ratio for all $j \in J$. The multiplier 10, simply scales $r(v)_j$ to a maximum value of 10. For nominal variables such as depth and hydraulic conductivity, they were first

Table 2 Description and original weights of the intrinsic and specific model parameters. Also given are the weights of the calibrated model, including the uncertainty ranges

| The DRASTIC model parameters | Parameter description | Original weight | Modified weight |
|--------------------------------|---|-----------------|-----------------|
| Depth to water (D) | Represents the depth from the ground surface to the water table. Deeper water table levels imply lesser contamination chances | 0.98 | (-0.23, 1.25) |
| Net recharge (R) | Represents the amount of water that penetrates the ground surface and reaches the water table. Recharge water represents the mean for transporting pollutants | 0.79 | (0.04, 1.35) |
| Aquifer media (A) | Refers to the material property of the saturated zone, which controls the pollutant attenuation processes | -0.16 | (-0.74, 1.08) |
| Soil media (S) | Represents the uppermost weathered portion of the unsaturated zone and controls the amount of recharge that can infiltrate downward | 2.76 | (0.96, 2.87) |
| Topography (T) | Refers to the slope of the land surface. It indicates the potential for runoff as opposed to infiltration | - | - |
| Impact of vadose zone (I) | Defines the material in the unsaturated zone. It controls the passage and attenuation of the contaminant to the saturated zone | 2.04 | (0.84, 2.54) |
| Hydraulic conductivity (C) | Indicates the ability of the aquifer to transmit water | 3 | (-0.15, 1.25) |
| Landuse (L) | Represents the effect of landuse activity on the aquifer | 5 | (0.92, 2.77) |

classified into several categories (based on Aller et al. 1987) and then the above equation was applied.

After rescaling the rates, the weights were optimized using the SUFI2 (Abbaspour et al. 2007) program of Soil Water Assessment Tool (SWAT)-CUP (Abbaspour 2007). SWAT-CUP was redesigned to run for DRASTIC. This program uses several methods to optimize a given objective function and it is available for use by other DRASTIC users upon request. SUFI2 performs model uncertainty and parameter sensitivity analysis as well as optimization. The objective function for optimization was defined as:

$$OF = \sum_{i=1}^n (V - [NO_3^-])^2 \tag{4}$$

where *OF* is the objective function, *V* is the vulnerability value (intrinsic or specific) ($mg\ l^{-1}$), $[NO_3^-]$ is the measured nitrate concentration in groundwater ($mg\ l^{-1}$) and *n* is the number of measured data. In SUFI2, weights were initially assigned a range of (0, 2). These ranges were then modified by the program by performing 500 simulations using Latin-hypercube sampling (McKay et al. 1979). Upon completion of the simulations, new parameter ranges were calculated (Abbaspour et al. 2007) and the process was repeated until no further improvement could be made to the objective function. As SUFI2 is a stochastic program, the final result is shown as 95% prediction uncertainty (95PPU). The goodness of calibration/uncertainty analysis is quantified by two parameters: *P*-factor and *R*-factor. *P*-factor quantifies the percentage of measured data bracketed by the 95PPU and has a maximum value of 1. *R*-factor quantifies the thickness of the 95PPU band with an ideal value approaching zero. The SUFI2 procedure tries to bracket most of the data within a narrow uncertainty band.

After each iteration, parameter sensitivities were determined by calculating the following multiple regression system, which regressed the Latin-hypercube-generated parameters against the objective function values:

$$g = \alpha + \sum_{i=1}^m \beta_i b_i \tag{5}$$

where α is the intercept, β_i is slope of the parameter, and *m* is the number of parameters. *t*-test was then used to identify the relative significance of each parameter.

Model parameterization

A short description of DRASTIC parameters is provided in Table 2. The basic database used to develop the model is as follows:

1. Depth to water table was obtained using data from 28 piezometers provided by HRWA. The water table

levels were subtracted from the elevation of the piezometer wells and averaged over a 6-year period (2001–2006). The depth to water table was then classified into ranges as defined by the DRASTIC model and assigned rates ranging from 1 (minimum impact on vulnerability) to 10 (maximum impact on vulnerability). The deeper the groundwater table, the smaller the rate. The water table layer was converted to raster format with 100-m cell size (Fig. 2a).

The net recharge layer was constructed using Piscopo method (Piscopo 2001):

$$\text{Recharge Index} = \text{Slope Index} + \text{Rainfall Index} + \text{Soil permeability Index} \tag{6}$$

First, a regional digital elevation model (DEM), provided by the National Cartographic Center of Iran, was generated with a spatial resolution of 20 m. After deriving the slopes, the slope was reclassified according to the criteria given in Table 3. Rainfall, permeability, and the resulting recharge indices were also calculated as specified in Table 3. Figure 2b shows the recharge map of the region.

Aquifer media information was obtained from the bore logs obtained from HRWA and the depth to water table. The raster map is shown in Fig. 2c. Aquifer media layer shows that most parts of the study area have the rating value equal to six (sand with silt and clay).

Soil map of the study area (1:50,000) was obtained from Hamadan Agricultural and Natural Resources Research Center. The soil classes of the study area were arranged based on the classes proposed by the DRASTIC method. As illustrated in Fig. 2d, most parts of the study area have rating value equal to four (silty loam).

The slope was calculated as stated in (2) above and classified based on Aller et al. 1987. This variable was removed from the calibration analysis as it was quite uniform for most of the region (Fig. 2e).

6. Impact of vadose zone layer (Fig. 2f) was constructed from the lithological cross-sections obtained from the geophysical data, bore logs and depth to water table data provided by HRWA.
7. To obtain the aquifer hydraulic conductivity map, transmissivity map was constructed using pumping test results provided by HRWA. The transmissivity values were converted to hydraulic conductivity using the aquifer thickness map obtained from HRWA. Figure 2g shows that most parts of the study area have hydraulic conductivity values ranging from 4 to 12 $m\ day^{-1}$.

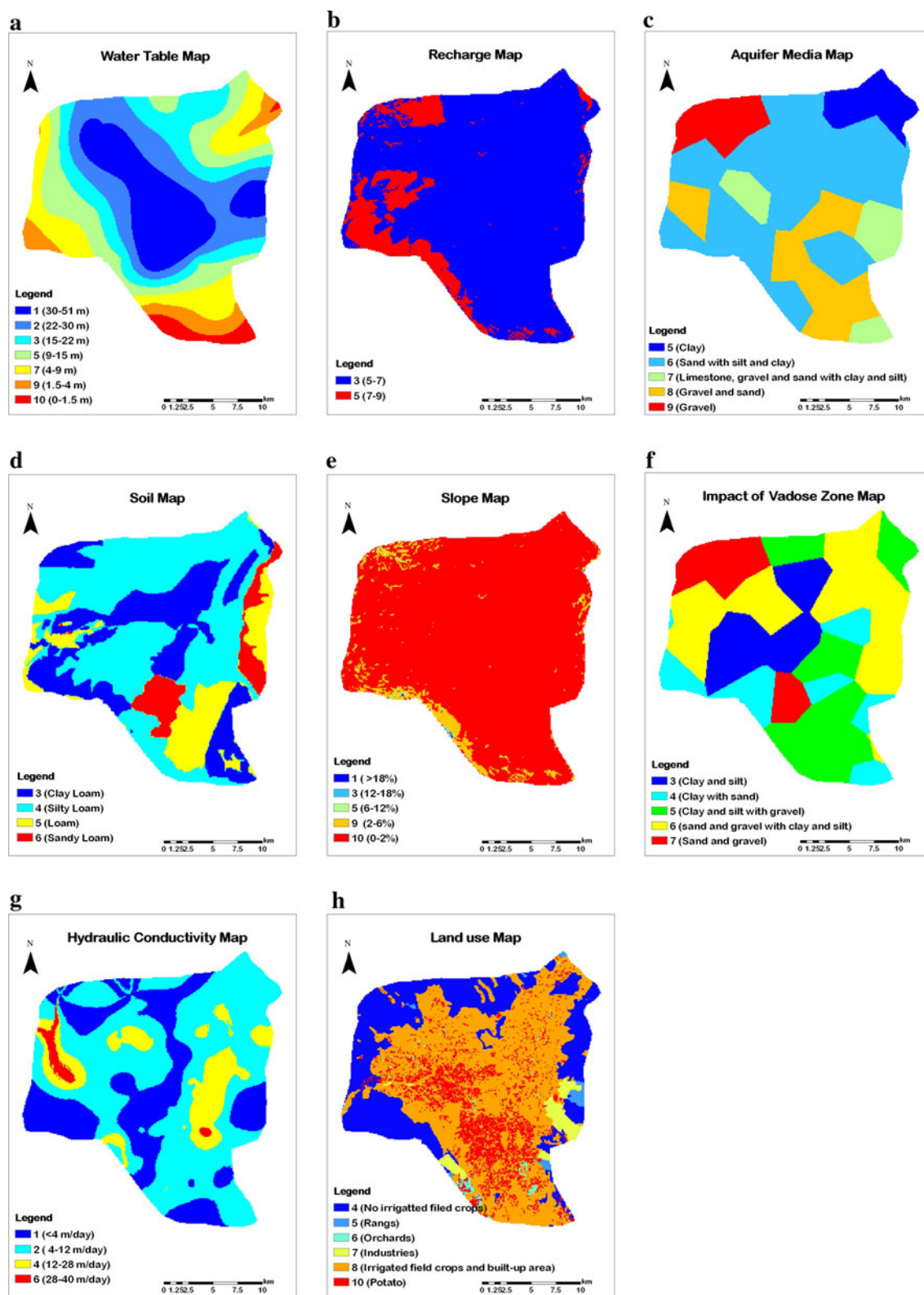


Fig. 2 Maps of DRASTIC parameter rates calculated for the Hamadan–Bahar plain

8. The data for the landuse map were prepared by classifying a LANDSAT-ETM⁺ satellite image taken on the year 2000 (<http://www.landsat.org>). For this study, ten categories of interest were classified using supervised maximum likelihood classification method with ENVI (2000) (Fig. 1). The reclassification of

Table 3 Description of slope, rainfall, and soil permeability indices used in the calculation of the recharge rates based on [RISOP](#) method

| Slope | | Rainfall | | Soil permeability | | Recharge value | |
|-----------|-------|-----------------------------------|-------|-------------------|-------|----------------|-------|
| Slope (%) | Index | Rainfall (mm year ⁻¹) | Index | Range | Index | Range | Index |
| <2 | 4 | >850 | 4 | High | 5 | 11–13 | 10 |
| 2–10 | 3 | 700–850 | 3 | Moderate to high | 4 | 9–11 | 8 |
| 10–33 | 2 | 500–700 | 2 | Moderate | 3 | 7–9 | 5 |
| >33 | 1 | <500 | 1 | Low | 2 | 5–7 | 3 |
| | | | | Very low | 1 | 3–5 | 1 |

Table 4 Original and modified rates of the specific vulnerability parameters

| Depth to water (D) | | | | Aquifer media (A) | | | |
|---|-----------------|--|--------------------|-----------------------------------|-----------------|--|--------------------|
| Range (m) | Original rating | Mean NO ₃ ⁻ (mg/l) | Conditioned rating | Aquifer type | Original rating | Mean NO ₃ ⁻ (mg/l) | Conditioned rating |
| 0–1.5 | 10 | 59.17 | 9 | Clay | 5 | 26.47 | 5 |
| 1.5–4 | 9 | 60.11 | 9 | Sand with silt and clay | 6 | 42.41 | 7 |
| 4–9 | 7 | 64.37 | 10 | Limestone, gravel, sand with clay | 7 | 35.035 | 6 |
| 9–15 | 5 | 55.52 | 9 | Gravel and sand | 8 | 58.25 | 10 |
| 15–23 | 3 | 27.23 | 4 | Gravel | 9 | 33.71 | 6 |
| 23–30 | 2 | 37.14 | 6 | | | | |
| 30–50 | 1 | 37.88 | 6 | | | | |
| Soil media (S) | | | | Impact of vadose zone (I) | | | |
| Soil type | Original rating | Mean NO ₃ ⁻ (mg/l) | Conditioned rating | Impact of vadose zone type | Original rating | Mean NO ₃ ⁻ (mg/l) | Conditioned rating |
| Clay loam | 3 | 27.37 | 4 | Clay and silt | 3 | 41.35 | 6 |
| Silty loam | 4 | 40.12 | 5 | Clay and sand | 4 | 40.33 | 6 |
| Loam | 5 | 76.79 | 10 | Clay, silt, with gravel | 5 | 64.10 | 10 |
| Sandy loam | 6 | 54.42 | 7 | Sand, gravel with clay and silt | 6 | 52.02 | 8 |
| | | | | Sand and gravel | 7 | 24.26 | 4 |
| Hydraulic conductivity of the aquifer (C) | | | | Landuse (L) | | | |
| Range (m/day) | Original rating | Mean NO ₃ ⁻ (mg/l) | Conditioned rating | Land use class | Original rating | Mean NO ₃ ⁻ (mg/l) | Conditioned rating |
| <4 | 1 | 39.77 | 8 | Non-irrigated field crops | 4 | 37.2 | 5 |
| 4–12 | 2 | 50.74 | 10 | Ranges | 5 | – | 5 |
| 12–28 | 4 | 31.25 | 6 | Orchards | 6 | 61.4 | 8 |
| 28–40 | 6 | – | 6 | Industries | 7 | 25.01 | 3 |
| | | | | Irrigated field crops | 8 | 44.91 | 6 |
| | | | | Built-up areas | 8 | 41.06 | 6 |
| | | | | Potato | 10 | 73.52 | 10 |

landuse for DRASTIC, however, resulted in six classes. Finally, groundwater samples were collected monthly in based on the procedure of [Secunda et al 1996](#) 37 wells across the region of study during fall 2007 to fall (Fig. 2h). For example, in this procedure “irrigated 2008. The monthly variations of nitrate concentration were field crops” and “buildup area” fall in the same class. quite small for the sampling period. Almost all ranges of

DRASTIC parameters were covered by the samplingshould decrease due to a faster moving groundwater and points. Plastic bottles were lled with the groundwater increased dilution. sample and the samples were analyzed forNO₃ by using a As it is usually done (Mohammadi et al2008), the DR/4000 Hach spectrophotometer. An independent nitrate intrinsic vulnerability scores of 69–152 obtained for the dataset containing measurements from a different set of 15 region were divided into ve classes (Table5). The wells was obtained from Rahman2003 and used for validation. The resulting vulnerability maps are illustrated in Fig. 3. Figure 3a shows that the intrinsic model predicts negligible and low vulnerability areas to be concentrated in the center of Hamadan–Bahar aquifer. This is partly due to the deep water table in this region, which has been precipitously lowered since 1976. In total, 54% of the area is rated as low and to negligible, 27% as moderate, and 17% as high vulnerability zones based on the intrinsic model. The speci c vulnerability map in Fig3b was constructed by combining the intrinsic vulnerability map and the potential pollution sources extracted from the landuse map. In the region, nitrate contamination of groundwater is believed to be mainly associated with intensive agricultural activities and to a lesser extent with urban landuse (Rahmani2003, Jalali2005, Nada an2007). The breakdown of the speci c vulnerability regions is given in Table5. It appears that introduction of landuse has increased the area of moderately vulnerable regions by 9%.

Results and discussion

In the rst phase of the analysis, the DRASTIC intrinsic andto negligible, 27% as moderate, and 17% as high vulnerability speci c vulnerability indices were calculated. Table shows the rates for all parameters. The weights are reported in Table2. An interesting observation with DRASTIC's s tructed by combining the intrinsic vulnerability map and speci cation of rates is the case of aquifer hydraulic con- the potential pollution sources extracted from the landuse ductivity. It is seen in Table4 that as conductivity increases, map. In the region, nitrate contamination of groundwater is rates also increase. Whereas one would expect that as con- ductivity increases, the potential for local contamination

activities and to a lesser extent with urban landuse (Rahmani2003, Jalali2005, Nada an2007). The breakdown of the speci c vulnerability regions is given in Table5. It appears that introduction of landuse has increased the area of moderately vulnerable regions by 9%.

Table 5 Intrinsic (speci c) vulnerability classes and the areas of groundwater pollution in Hamadan–Bahar plain

| DRASTIC index | Vulnerability range | Area (km ²) | Area (%) |
|---------------|-----------------------------|-------------------------|----------|
| Negligible | 69–86 (94–119) ^a | 77 (33) | 16 (7) |
| Low | 86–103 (119–132) | 187 (181) | 38 (37) |
| Moderate | 103–119 (132–145) | 132 (175) | 27 (36) |
| High | 119–135 (145–160) | 85 (88) | 17 (18) |
| Extreme | 135–152 (160–192) | 5 (9) | 1 (2) |

^a Numbers *inbrackets* are based on speci c vulnerability model

To test the performance of the intrinsic and speci c DRASTIC maps in predicting aquifer nitrate contamination, we also plotted all measured nitrate concentration in Fig. As shown, the larger nitrate concentrations are more or less in the predicted high vulnerability zones, but a few wells within the low vulnerability zones also have large nitrate concentrations. While visually, there seems to be a good relationship between nitrate concentration in Hamadan–

Fig. 3 a Intrinsic vulnerability andb speci c vulnerability maps. Also shown is the measured nitrate concentration in the wells for calibration (*brown*) and validation (*pink*) datasets. The number refers to the scale of the bars

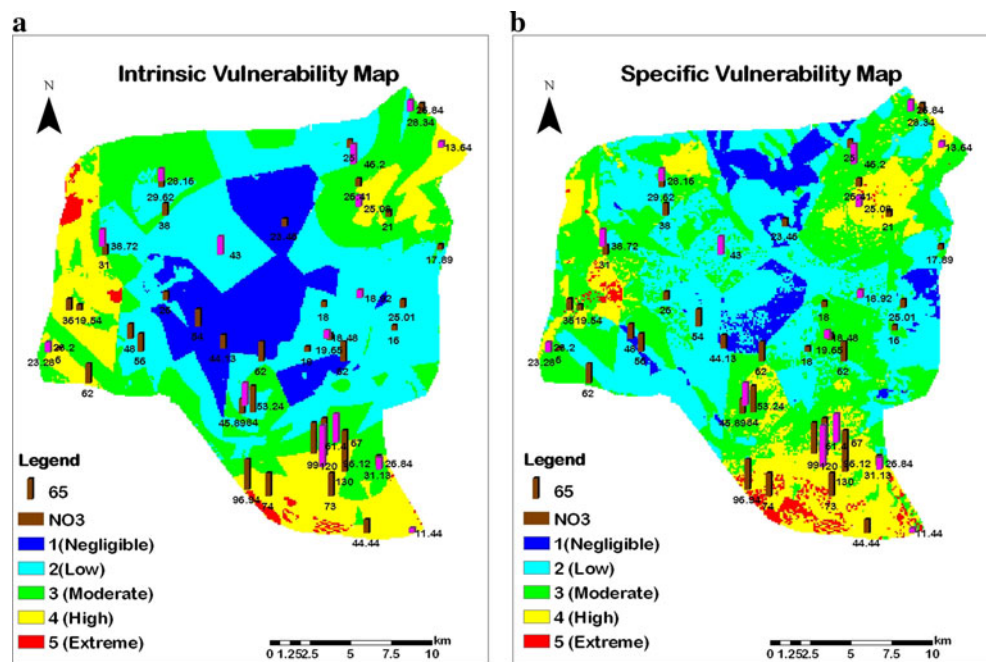


Table 6 Statistics of goodness of fit for different models

| Model | R-factor | P-factor | R ² | MSE |
|--|----------|----------|----------------|-------|
| Intrinsic | – | – | 0.12 | 3,289 |
| Specific | – | – | 0.19 | 8,169 |
| Specific with optimized weights | 1.05 | 0.57 | 0.27 | 731 |
| Conditioned model rates with optimized weights | 1.19 | 0.68 | 0.52 | 570 |
| Validation data set | 1.67 | 0.67 | 0.51 | 312 |

Table 7 Correlation coefficient of measured nitrate and rates of specific and conditioned vulnerability parameters

| | NO ₃ | D | R | A | S | I | C | L |
|-----------------|------------------------|------------|-------------|-------------|------------|-----------|-----------|-----|
| NO ₃ | 1.0 | | | | | | | |
| D | 0.3 (0.4) ^a | 1.0 | | | | | | |
| R | –0.1 (–0.1) | 0.4 (0.2) | 1.0 | | | | | |
| A | 0.2 (0.3) | –0.3 (0.2) | –0.1 (0.0) | 1.0 | | | | |
| S | 0.4 (0.6) | –0.3 (0.2) | –0.3 (–0.2) | 0.3 (0.4) | 1.0 | | | |
| I | 0.0 (0.5) | –0.3 (0.3) | –0.2 (–0.2) | 0.4 (0.4) | 0.5 (0.3) | 1.0 | | |
| C | –0.1 (0.3) | –0.1 (0.2) | –0.1 (0.1) | –0.1 (–0.1) | –0.1 (0.4) | 0.1 (0.2) | 1.0 | |
| L | 0.3 (0.4) | –0.1 (0) | –0.4 (–0.3) | 0.2 (0.1) | 0.2 (0.2) | 0.2 (0.3) | 0.2 (0.0) | 1.0 |

^a Numbers in brackets are correlations of the conditioned model

Bahar aquifer and the DRASTIC vulnerability maps, but weak as indicated in Table 7 and the near- at slope of the statistically, the R² values are only 0.12 and 0.19, respectively, for intrinsic and specific models (Table 6). One largest correlations with nitrate. Soil was also found to be possible reason for the poor correlation is that the DRASTIC method accounts for the ease of the vertical movement of the aquifer system (Almasri and Doolittle 1998). Aquifer hydraulic conductivity, recharge, and contaminants to the water table without any explicit vadose zone impact exhibited the poorest correlation with accounting of possible fate and transport of nitrate in the soil and aquifer system (Almasri and Doolittle 2008). For example, it is well known that macropore (or preferential) flow could deliver large amounts of contaminants to deep aquifers by bypassing much of the soil matrix (Tyner et al. 2007; Moradi et al. 2005). This process would make the depth to water table and variable insignificant. Given the importance of the landuse variable, the improvement in the specific model when conditioned rates, the correlation with nitrate has increased while compared with the intrinsic one was smaller than expected the correlation between the parameters has decreased. The Interestingly, the mean square error (MSE) for the specific model increased quite significantly (Table 6). Panagopoulos et al. (2006) also did not find much improvement by adding the landuse variable. They argued that the points with a high intrinsic vulnerability also have high contaminant loadings, as it is the case in our study area. clay and silt” play a more important role in transferring and identifying nitrate-contaminated zones, the correlations were found to be less important for nitrate flow than “clay variables were calculated as shown in Table 4 and silt” indicating the influence of macropore flow in also illustrates graphs of nitrate concentrations and nitrate movement as a result of cracking due to shrinkage. DRASTIC rates (black curves). For ease of observation, we sorted the data with increasing nitrate concentrations and plotted the trend line for DRASTIC rates. Figure 4 shows that there is much variability in the parameter rates and the correlation with nitrate concentration is generally used to optimize the parameter weights considering the

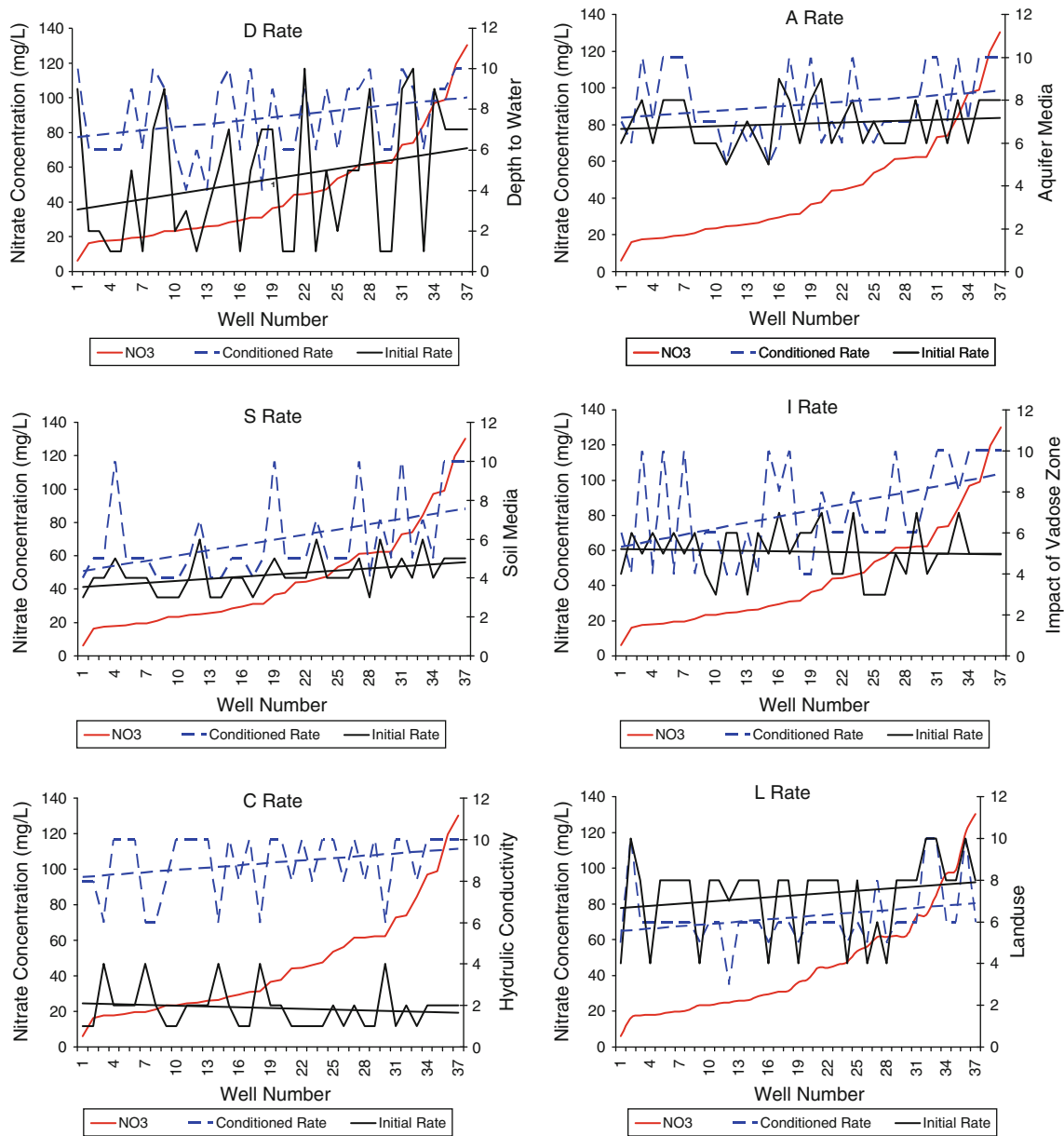


Fig. 4 Graphs showing sorted nitrate concentration and the corresponding rates for different DRASTIC parameters. Also shown is the trend line for the rates. Black curves represent the rates of the original DRASTIC model, while blue curves are the conditioned rates

objective function in Eq. 4. Table 6 shows the pertinent statistics of calibration and validation results. Ideally, the P -factor should approach 1 and the R -factor should approach zero. Validation data set has a larger P -factor (with a similar coverage of the measured points) than the calibration data set. The MSE is, however, also quite smaller for the validation database. The values of the best simulations for validation and calibration were 0.52 and 0.51, respectively (Table 6).

Parameter sensitivities are determined by calculating multiple regression system in SUFI2; this provides partial information about the sensitivity of the objective function

to model parameters. In the study, the objective function was found to be sensitive to soil media, impact of vadose zone, hydraulic conductivity, recharge, land use, aquifer media, and depth to water, in order of importance.

The modified vulnerability map is plotted in Fig. 5. This map provides direct nitrate concentrations instead of vulnerability index. Large nitrate concentration areas are much better depicted in this map. The Hamadan drinking water standard for nitrate is 45 mg l^{-1} . According to

Fig. 5, nitrate concentration below the standard was detected in 60% of the study area, while 40% have concentrations above the standard. Fig. 6 shows a nitrogen

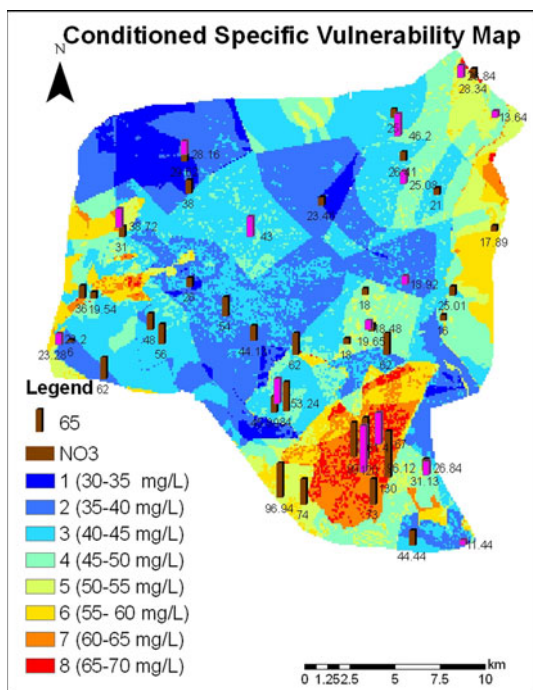


Fig. 5 The vulnerability map for the conditioned model. Also shown is the measured nitrate concentration in the wells for calibration (brown) and validation (pink) datasets

enters the region from the south. More studies are needed to determine the share of each source in contaminating the groundwater system.

Based on the existing reports, groundwater discharges and the evolving number of wells in the region are presented in Table 8. Figure 6 shows the water table status in 1976 and the one averaged over a 6-year period in 2001–2006. There has been a tremendous rise in the number of wells withdrawing water from the aquifers and a drastic drop in the water table in the central plain of Hamadan–Bahar. This has undoubtedly created a complex regional flow system. The DRASTIC models show small vulnerability in the central plain mainly because the groundwater table is quite deep. But in reality, the vulnerability of this region should be quite large because groundwater gradient should now be directed towards the central valley bringing in polluted water from all sides. More groundwater samples in the central plain may, therefore, reveal a different contamination picture.

For a comparison with the present condition, in Fig. 7 the intrinsic vulnerability map of 1976 was plotted. All DRASTIC parameters between the past and the present should have remained fairly constant, except for the depth to water table. The greatest change between the two periods is in the central part of the plain, spatially from south to north following the direction of groundwater flow west to north-east. The water table in the central region was quite high in 1976; hence DRASTIC calculates a larger vulnerability. In 1976, about 39% of the region was predicted to have a high intrinsic vulnerability, while the current prediction puts this number at around 17%. This reduction is entirely due to declining water table in the central valley. But in reality, macropore flow can more than compensate for the lowering of water table in delivering contaminants to groundwater.

As groundwater table is higher in the regions surrounding the valley than in the middle of the Hamadan–Bahar plain, a reversal of flow gradient towards the center is expected, which will bring in polluted groundwater from the north, south, and west. The central valley is, hence, a danger zone, which needs to be carefully monitored.

Table 8 Temporal changes in the number of wells and groundwater discharge in Hamadan–Bahar aquifer

| Year | Deep wells | | Semi-deep wells | | Qanats | | Springs | | Total discharge (MCM) |
|------|------------|-----------------|-----------------|-----------------|--------|-----------------|---------|-----------------|-----------------------|
| | Number | Discharge (MCM) | Number | Discharge (MCM) | Number | Discharge (MCM) | Number | Discharge (MCM) | |
| 1976 | 9 | 4 | 692 | 97 | 43 | 29 | – | – | 130 |
| 1991 | 991 | 248 | 1,287 | 66 | 107 | 19 | 121 | 13 | 346 |
| 2003 | 1,024 | 228 | 1,250 | 71 | 111 | 31 | 327 | 8 | 339 |

MCM million cubic meters

Fig. 6 The map of depth to groundwater table in 1976 and b averaged over 2001–2006

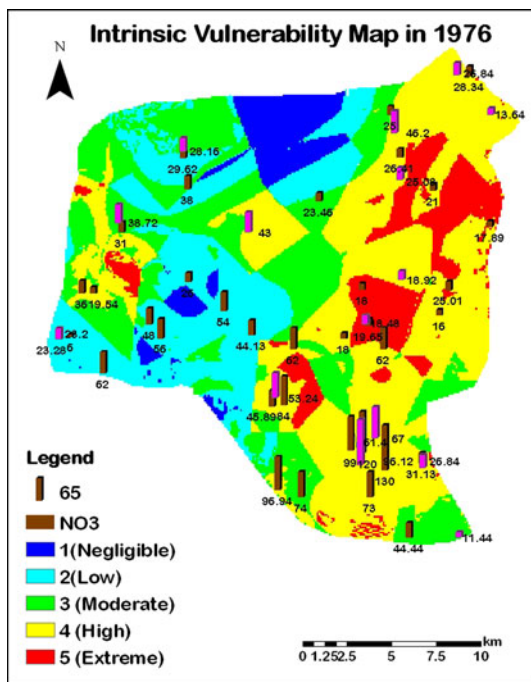
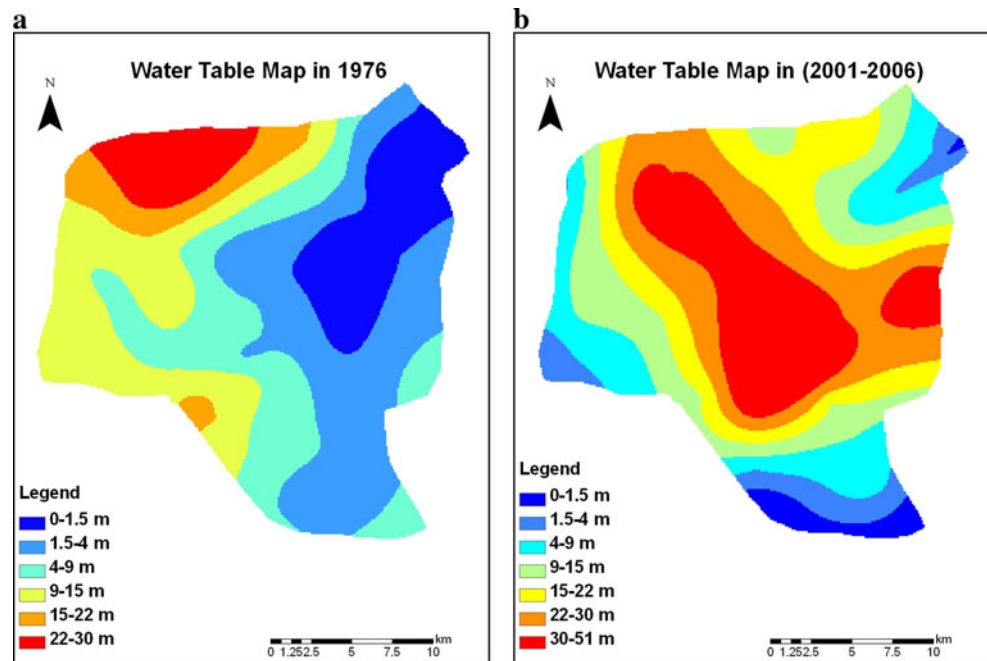


Fig. 7 DRASTIC vulnerability map based on the 1976 groundwater depth data

Conclusions

This study confirmed that training of DRASTIC model rates based on measured nitrate concentrations significantly improves model's ability to delineate vulnerable sites. Although the number of measured data in the calibration data set was small, but the favorable results of the independent validation dataset did not show severe over fitting

of the parameters. In a following study, we will consider modeling the region with SWAT (Arnold et al 1998) hydrologic simulator and implementation of alternative BMPs to alleviate the aquifer nitrate problems.

Acknowledgments The authors wish to acknowledge Hamadan Regional Water Authority, Water and Wastewater Co. of Hamadan, Isfahan University of Technology, and the Swiss Federal Institute for Aquatic science and Technology, Eawag, for providing assistance to conduct this study.

References

- Abbaspour KC (2007) User manual for SWAT-CUP, SWAT calibration and uncertainty analysis programs. Swiss Federal Institute of Aquatic Science and Technology, Eawag, Dürdorf, Switzerland. http://www.eawag.ch/organisation/abteilungen/siam/software/swat/index_E Accessed Aug 2009
- Abbaspour KC, Yang J, Maximov I, Siber R, Bogner K, Mieleitner J, Zobrist J, Srinivasan R (2007) Modelling hydrology and water quality in the pre alpine/alpine Thur watershed using SWAT. *J Hydrol* 333:413–430
- Al-Adamat RAN, Foster IDL, Baban SMJ (2003) Groundwater vulnerability and risk mapping for the Basaltic aquifer of the Azraq basin of Jordan using GIS, remote sensing and DRASTIC. *Appl Geogr* 23:303–324
- Aller L, Bennett T, Lehr JH, Petty RJ, Hackett G (1987) DRASTIC: a standardized system for evaluating ground water pollution potential using hydrogeologic settings. EPA-600/2-87-035, EPA, Washington
- Almasri MN (2008) Assessment of intrinsic vulnerability to contamination for Gaza coastal aquifer, Palestine. *J Environ Manage* 88(4):577–593
- Arnold JG, Srinivasan R, Muttiah RS, Williams JR (1998) Large area hydrologic modeling and assessment—Part 1: model development. *J Am Water Resour Assoc* 34:73–89

- Babiker IS, Mohamed AAM, Hiyama T, Kato K (2005) A GIS based DRASTIC model for assessing aquifer vulnerability in Kakami-gahara Heights, Gifu Prefecture, Central Japan. *Sci Total Environ* 345(1–3):127–140
- Chitsazan M, Akhtari Y (2008) A GIS-based DRASTIC model for assessing aquifer vulnerability in Kherran plain, Khuzestan, Iran. *Water Resour Manage*. doi:10.1007/s11269-008-9319-8
- Garrett P, Williams JS, Rossoll CF, Tolman AL (1989) Are ground water vulnerability classification systems workable? In: Proceedings of FOCUS conference on eastern regional ground water issues, Kitchener, Ontario, Canada, National Water Well Association, Dublin, Ohio, 17–19 October, pp 329–343
- Gogu RC, Dassargues A (2000) Current trends and future challenges in groundwater vulnerability assessment using overlay and index methods. *Environ Geol* 39(6):549–559
- Hamza MH, Added A, Rodriguez R, Abdeljaoueda S, Ben Mammou A (2007) A GIS-based DRASTIC vulnerability and net recharge reassessment in an aquifer of a semi-arid region (Metline-Ras Jebel-Raf Raf aquifer, Northern Tunisia). *J Environ Manage* 84:12–19
- Jalali M (2005) Nitrates leaching from agricultural land in Hamadan, western Iran. *Agric Ecosyst Environ* 110:210–218
- Kalinski RJ, Kelly WE, Bogardi I, Ehrman RL, Yamamoto PO (1994) Correlation between DRASTIC vulnerabilities and incidents of VOC contamination of municipal wells in Nebraska. *Ground Water* 32(1):31–34
- McKay MD, Beckman RJ, Conover WJ (1979) A comparison of three methods for selecting values of input variables in the analysis of output from a computer code. *Technometrics* 21:239–245
- McLay CDA, Dragden R, Sparling G, Selvarajah N (2001) Predicting groundwater nitrate concentrations in a region of mixed agricultural land use: a comparison of three approaches. *Environ Pollut* 115:191–204
- Merchant J (1994) GIS-based groundwater pollution hazard assessment: a critical review of the DRASTIC model. *Photogramm Eng Remote Sens* 60(9):1117–1127
- Mohammadi K, Niknam R, Majd VJ (2008) Aquifer vulnerability assessment using GIS and fuzzy system: a case study in Tehran–Karaj aquifer, Iran. *Environ Geol*. doi:10.1007/s00254-008-1514-7
- Moradi A, Abbaspour KC, Afyuni M (2005) Modelling field-scale cadmium transport below the root zone of a sewage sludge amended soil in an arid region in Central Iran. *J Contam Hydrol* 79(3–4):187–206
- Nadani H (2007) Simulation of groundwater pollution around drinking water wells in Hamadan city. M.Sc. dissertation, Shahid Beheshti University, Tehran, Iran
- Palmer RC, Lewis MA (1998) Assessment of groundwater vulnerability in England and Wales. In: Robins NS (ed) *Groundwater pollution, aquifer recharge and vulnerability*, special publications vol 130. Geological Society, London, pp 191–198
- Panagopoulos GP, Antonakos AK, Lambrakis NJ (2006) Optimization of DRASTIC model for groundwater vulnerability assessment, by the use of simple statistical methods and GIS. *Hydrogeol J* 14:894–911
- Piscopo G (2001) In: *Groundwater vulnerability map, explanatory notes, Castlereagh Catchment, NSW*. Department of Land and Water Conservation, Australia. http://www.dwe.nsw.gov.au/water/pdf/quality_groundwater_castlereagh_map_notes.pdf. Accessed Aug 2008
- Rahman A (2008) A GIS-based DRASTIC model for assessing groundwater vulnerability in shallow aquifer in Aligarh, India. *Appl Geogr* 28:32–53
- Rahmani A (2003) Study and investigation of pollution in groundwater of Hamadan-Bahar plain. Environmental Organization of Hamadan, Iran
- Rosen L (1994) A study of the DRASTIC methodology with emphasis on Swedish conditions. *Ground Water* 32:278–285
- Secunda S, Collin M, Melloul AJ (1998) Groundwater vulnerability assessment using a composite model combining DRASTIC with extensive land use in Israel's Sharon region. *J Environ Manage* 54:39–57
- Tyner JS, Wright WC, Yoder RE (2007) Identifying long-term preferential and matrix flow recharge at the field scale. *T ASABE* 50(6):2001–2006
- Villeneuve JP, Banton O, Lafrance P (1990) A probabilistic approach for the groundwater vulnerability to contamination by pesticides: the VULPEST model. *Ecol Model* 51:47–58
- Vrba J, Zaporozec A (1994) *Guidebook on mapping groundwater vulnerability*, vol 16. International Association of Hydrogeologists, Heise